
MESHES MEET VOXELS: ABDOMINAL ORGAN SEGMENTATION VIA DIFFEOMORPHIC DEFORMATIONS

Fabian Bongratz^{1,3}, Anne-Marie Rickmann^{1,2}, Christian Wachinger^{1,2,3}

¹ Department of Radiology, Technical University of Munich

² Department of Child and Adolescent Psychiatry, Ludwig-Maximilians-University Munich

³ Munich Center for Machine Learning

{fabi.bongratz, christian.wachinger}@tum.de, arickman@med.lmu.de

ABSTRACT

Abdominal multi-organ segmentation from CT and MRI is an essential prerequisite for surgical planning and computer-aided navigation systems. Three-dimensional numeric representations of abdominal shapes are further important for quantitative and statistical analyses thereof. Existing methods in the field, however, are unable to extract highly accurate 3D representations that are smooth, topologically correct, and match points on a template. In this work, we present UNetFlow, a novel diffeomorphic shape deformation approach for abdominal organs. UNetFlow combines the advantages of voxel-based and mesh-based approaches for 3D shape extraction. Our results demonstrate high accuracy with respect to manually annotated CT data and better topological correctness compared to previous methods. In addition, we show the generalization of UNetFlow to MRI.

1 Introduction

The goal of medical image segmentation is to extract anatomical structures in the image. Despite the progress in tomographic imaging, the image resolution of CT and MRI is typically in the order of millimeters. Hence, even accurately predicted segmentation, as well as manual annotations, can only approximate the actual organ contour since they are limited to the voxel grid. The consequence are stair-case artifacts shown in Figure 1. While voxel segmentations are sufficient for coarse morphological analyses, fine-grained geometric analyses of organs and clinical navigation systems need highly accurate segmentations of organ boundaries [1].

With 3D meshes, we can overcome the limitations of the voxel grid by having an explicit representation of the contour, see Figure 1. 3D meshes are a natural representation of shapes as they can capture the topology and smoothness of the organ surfaces. However, current deep mesh-based shape extraction methods require complex neural architectures and an involved combination of loss functions [2, 3, 4] or are not trainable in an end-to-end fashion [5, 6]. Moreover, these methods are usually not designed for working with multiple shapes and can therefore not learn relations among them. On the other hand, voxel-based methods can easily segment multiple anatomical structures from 3D images, but they lack important properties such as topological correctness, smoothness, and point correspondence, i.e., they do not carve out shape characteristics as well as meshes.

We propose *UNetFlow*, which combines the advantages of both voxel-based and mesh-based approaches for 3D shape extraction of abdominal organs. UNetFlow consists of a single multi-task UNet that *simultaneously* outputs voxel masks and mesh coordinates for each organ. The mesh coordinates are computed by a diffeomorphic template deformation, establishing a point-wise correspondence of surface points. UNetFlow does not require any manual correspondences or landmark points as input, as it learns to generate consistent and homologous meshes across different subjects. We evaluate UNetFlow on a large dataset of 1,000 abdominal CT scans [7] and a smaller MRI dataset (70 scans) with annotations for four organs: kidneys, liver, pancreas, and spleen. We compare our method with existing mesh-based methods in terms of segmentation accuracy, topological correctness, and transfer learning. Our results show that

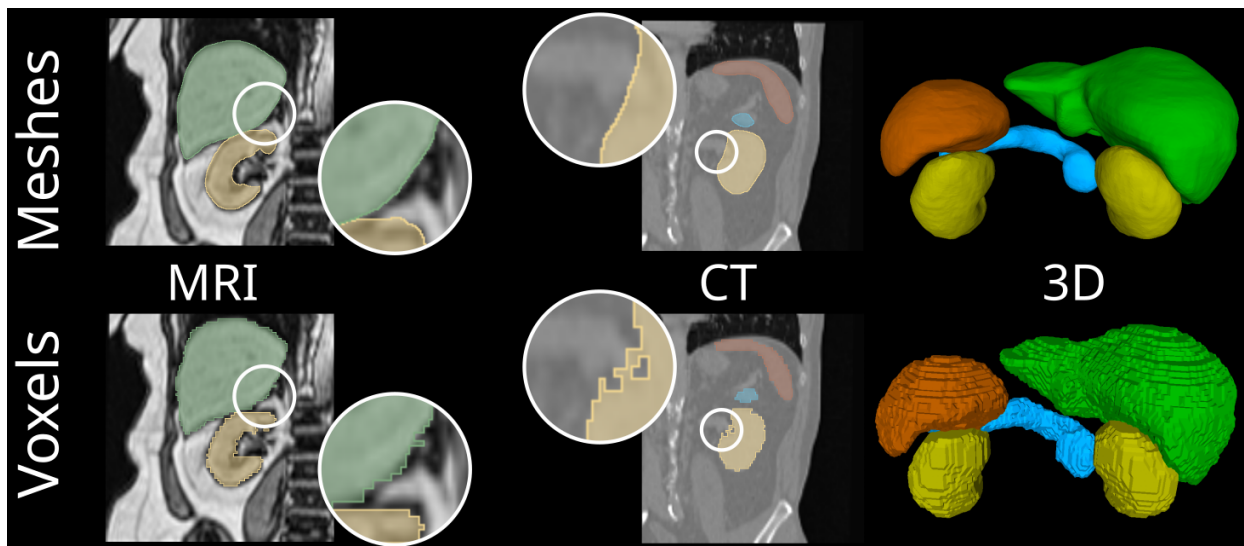


Figure 1: Meshes (top, computed with UNetFlow on our MRI and CT test sets) represent shape characteristics of abdominal organs, i.e., smooth surface morphology and spherical topology, better than voxel maps (bottom), as visualized for MRI, CT, and a 3D surface rendering.

UNetFlow achieves state-of-the-art performance in segmentation, while being computationally efficient and easy to implement.

In summary, our main contributions are the following:

- We design an efficient, easy-to-use neural network for multi-organ shape reconstruction from 3D scans of the abdomen. It is based on a single multi-task UNet and learns a diffeomorphic mapping from an input template to the output shapes as well as a voxel segmentation.
- We propose an effective, registration-based post-processing step that aligns the predicted shapes to the segmentation output to enforce the consistency of the shapes with the voxel segmentation.
- Using a large public CT dataset and a smaller MRI dataset, we demonstrate that UNetFlow yields state-of-the-art surface meshes of four abdominal organs in terms of accuracy and topological measures.

Related work Voxel-based biomedical segmentation has seen unprecedented advances in recent years, especially since the advent of the UNet architecture [8] and its variants [9, 10, 11]. These methods, however, are limited by the voxel resolution and the identification of homologous surface points is particularly difficult [12]. On the other hand, previous work has introduced deep learning-based methods that are capable of *directly* computing surface meshes from a 2D [13, 14] or 3D [2, 4, 5] input image via template deformation. In this work, we bridge the gap between these two fields by presenting a mesh-based segmentation method that aligns the predicted shapes to a voxel segmentation, eventually achieving higher accuracy while preserving all advantages of direct mesh reconstruction.

2 Method

In the following, we describe the details of UNetFlow, a novel method for the simultaneous reconstruction of multiple anatomical shapes from 3D medical data with point correspondence to a template. Figure 2 depicts an overview.

2.1 Voxel space

At its core, we employ a 3D residual UNet based on the 3D-full-resolution network implemented in [11]. This fully-convolutional neural network projects a 3D input scan into a low-resolution latent space. From the latent space, the decoder recovers the original image size in a step-wise manner, producing a stack of cuboidal feature maps with increasing resolution. From the final UNet layer, a segmentation is obtained via Softmax activations. To improve training convergence, we compute the segmentation (cross entropy) loss \mathcal{L}_{CE} not only from the final UNet output but also from intermediate decoder layers [15].

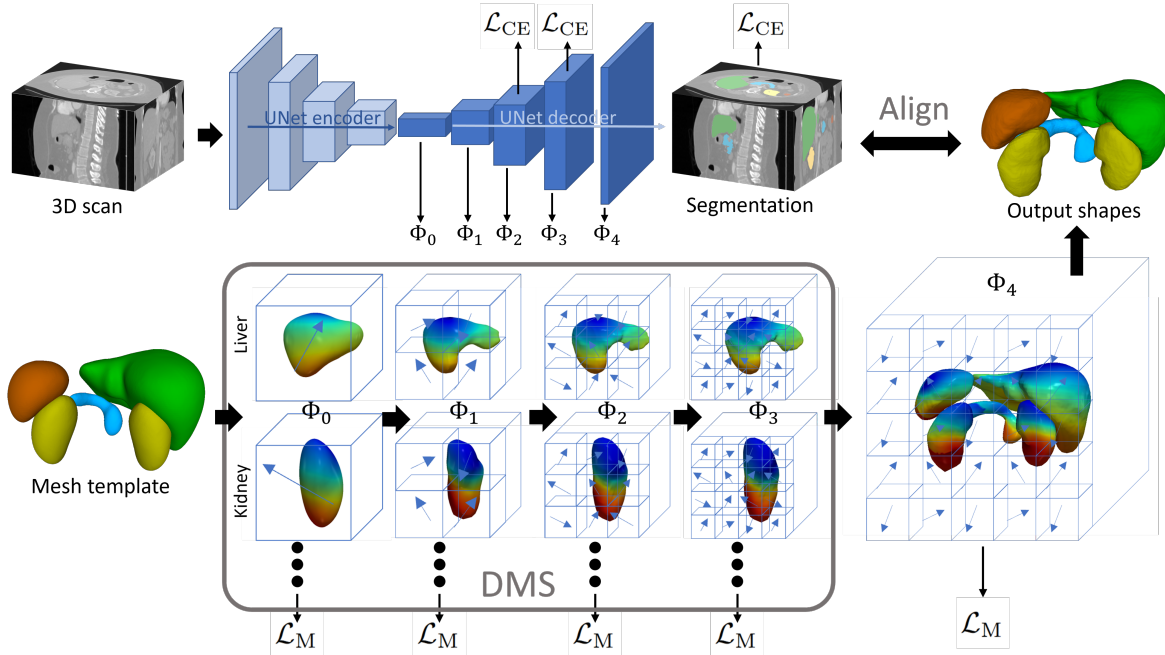


Figure 2: Architecture of UNetFlow. The predicted flow fields Φ_{0-4} enable a correspondence-preserving deformation of the input template, guided via deep mesh supervision (DMS). The model is trained in a multi-task setting via a combination of voxel (\mathcal{L}_{CE}) and mesh loss (\mathcal{L}_M). At test time, the consistency of the output shapes with the segmentation is ensured via surface registration.

2.2 Neural flow fields and deep mesh supervision

The lower part of Figure 2 is dedicated to the deformation of the mesh template $\mathcal{T} \subset \mathbb{R}^3$. From a high-level view, UNetFlow computes an (approximately) diffeomorphic deformation, i.e., an invertible mapping $f: \mathbb{R}^3 \rightarrow \mathbb{R}^3$, from the template to the output shapes. Throughout this work, we assume that each *mesh* can be subdivided into K connected components (CCs). That is, each CC defines the boundary of one of K abdominal organs and is (approximately) homeomorphic to the sphere $S^2 = \{x \in \mathbb{R}^3 : \|x\|_2 = 1\}$ (meshes may contain self-intersections, cf. Section 3.2).

Inspired by recent advances in neural shape deformations [16, 5], we model the deformation of the mesh template via an ordinary differential equation (ODE). Formally, the trajectory of any surface point $x \in \mathcal{T}$ is described by

$$\frac{dx(t)}{dt} = \Phi(x(t), t), \quad x(t=0) = x_T, \quad (1)$$

where x_T is the initial location on the template, i.e., the boundary condition of the ODE. Figuratively, Φ is a flow field in Euclidean space that acts on the surface points and causes a deformation of the template. This framework has a strong theoretical foundation since the solution to Equation (1) represents a diffeomorphic mapping between surface points [5] and thereby naturally avoids self-intersections during the deformation. In order to solve Equation (1), any numerical black-box solver can be applied. In our implementation, we stick to an Euler integration scheme as it is fast, efficient in terms of memory, and easy to implement.

While, in general, Φ is time-varying, we define it to be mostly constant and to only change at discrete equidistant time points t_i . Without loss of generality, we assume $t_i \in \mathbb{N}_0$, so that

$$\Phi(x(t), t) = \Phi_{\lfloor t \rfloor}(x(t)), \quad (2)$$

where $\{\Phi_i : i = 0, \dots, 4\}$ is a set of five stationary flow fields. In contrast to previous work [5, 6], where each Φ_i is parameterized by a separate UNet, we compute Φ_{0-4} directly from the feature maps of a single UNet decoder (see Figure 2). This makes the network end-to-end trainable and more efficient in terms of parameters. Moreover, the “resolution” of each flow field is equal to the resolution of the feature map at the respective decoder stage. Thereby, the level of detail in the reconstruction is increased gradually from coarse to fine, ultimately enabling a higher reconstruction accuracy with better topological measures, cf. Sections 3.1 and 3.2. From the final and intermediate meshes, we compute a mesh loss \mathcal{L}_M , which consists of a Chamfer and an edge-length term ($\lambda = 10$) implemented in [17]. This *deep mesh supervision* (DMS) is expected to increase robustness and generalization of the geometric reconstructions [18].

Table 1: UNetFlow outperforms previous mesh-based surface extraction algorithms on the CT test set ($n = 147$). We report Dice scores and average symmetric surface distance (ASSD) with respect to the ground-truth annotations per organ (mean \pm sd). Best values are **highlighted**.

Method	Kidneys		Liver	
	Dice \uparrow	ASSD (mm) \downarrow	Dice \uparrow	ASSD (mm) \downarrow
<i>V2M</i> [2]	0.83 \pm 0.09	1.92 \pm 2.33	0.94 \pm 0.04	1.86 \pm 1.52
<i>CF</i> [5]	0.88 \pm 0.13	2.31 \pm 4.01	0.95 \pm 0.06	1.90 \pm 1.80
<i>V2C</i> [4]	0.90 \pm 0.09	1.60 \pm 2.52	0.95 \pm 0.04	1.68 \pm 1.66
UNetFlow	0.92 \pm0.07	1.22 \pm2.19	0.96 \pm0.03	1.39 \pm1.07
Method	Pancreas		Spleen	
	Dice \uparrow	ASSD (mm) \downarrow	Dice \uparrow	ASSD (mm) \downarrow
<i>V2M</i> [2]	0.54 \pm 0.12	4.07 \pm 3.42	0.84 \pm 0.11	2.16 \pm 3.22
<i>CF</i> [5]	0.57 \pm 0.18	5.63 \pm 4.84	0.90 \pm 0.14	2.23 \pm 4.44
<i>V2C</i> [4]	0.72 \pm0.15	3.88 \pm 4.26	0.91 \pm 0.10	1.67 \pm 3.20
UNetFlow	0.71 \pm 0.19	3.58 \pm3.90	0.93 \pm0.10	1.43 \pm4.64

2.3 Multi-task learning

While most previous mesh-based surface extraction methods are limited to single shapes, UNetFlow can handle an arbitrary number of organs in parallel. To this end, we predict a separate deformation field for each organ in all of the intermediate deformation stages. In the final stage, i.e., Φ_4 , however, we deform all shapes with a single deformation field. As confirmed by Figure 3, this prevents organ boundaries to intersect in regions where two organs lie very close together or even touch each other superficially (e.g., the liver and the right kidney). In addition, we propose to align the predicted meshes to the voxel output via surface registration [19]. As can be deduced from our ablation study (Table 2), this post-processing is effective in that it improves mesh accuracy while preserving topological properties and template correspondence.

3 Results

The two imaging modalities in our experiments are CT and MRI. For CT images, we used the public AbdomenCT-1K dataset [7]¹, which contains 1,000 abdominal CT scans with manual annotations for four organs: kidneys, liver, spleen, and pancreas. After excluding scans with missing organs, we split the CT data into train, validation, and test splits with 666, 167, and 147 scans, respectively. CT images were z-score normalized. For MRI scans, we used Dixon opposed-phase (OPP) images from three different datasets: UKBiobank [20] (37 scans), GNC [21] (16 scans), and KORA [22] (17 scans). The OPP images were pre-processed following the steps from [23], which involves bias field correction, resampling, cropping, and annotation by an anatomy expert. Our MRI training, validation, and test splits contained 47, 5, and 18 samples, respectively, balanced according to data sources. MRI images were min-max normalized. For all images, we performed affine registration [24] to a randomly selected reference image² to ensure spatial alignment ($2 \times 2 \times 3 \text{mm}^3$ resolution). Finally, we extracted ground truth meshes for each organ from the label masks using marching cubes [25].

3.1 Reconstruction accuracy

Comparison to the state-of-the-art We compare UNetFlow to three recent state-of-the-art mesh reconstruction methods that start from an initial template: Voxel2Mesh (*V2M*) [2], CorticalFlow (*CF*) [5], and Vox2Cortex (*V2C*) [4]. We adapted all baseline methods to multi-organ segmentation and used a consistent template created from the average organ shapes in our CT training set. The only exception was for *V2M*, which comes with spherical templates. We report Dice scores and surface accuracy on the CT test set in Table 1 and notice that UNetFlow’s performance is superior to the shown baselines. At the same time, UNetFlow is simpler to use than *V2M/V2C* (fewer loss functions, simpler architecture) and more efficient in terms of computational resources compared to *CF* (one instead of three UNets, end-to-end learning of all organs). Moreover, Figure 3 illustrates that UNetFlow avoids typical pitfalls of previous approaches when assessing the visual quality of delineated organ boundaries. Most importantly, UNetFlow is able to

¹<https://github.com/JunMa11/AbdomenCT-1K>

²Case_00001 from AbdomenCT-1K, excluded from the test set

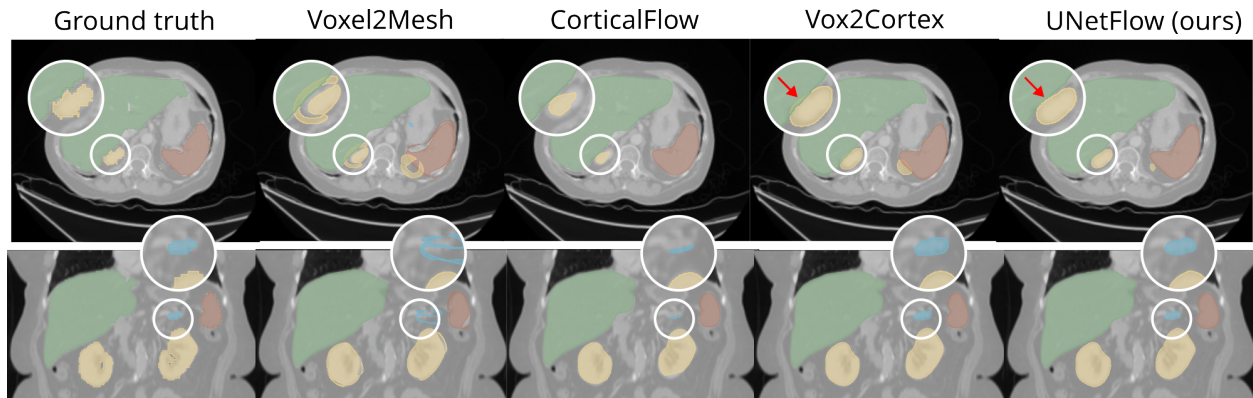


Figure 3: UNetFlow avoids typical pitfalls of previous mesh-based organ extraction methods. Shown is a qualitative comparison of segmentation slices from two subjects of the CT test set together with the respective ground truth annotation.

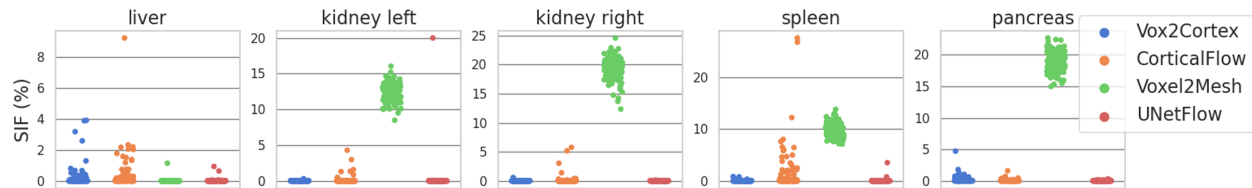


Figure 4: Quantitative analysis of topological correctness of extracted organs on our CT test set in terms of self-intersecting faces (SIF) per organ.

correctly separate the liver and the right kidney in the shown slice (red arrows), which we attribute to our final fused deformation field Φ_4 . Due to its compact architecture, UNetFlow only takes 0.08s for a forward pass on an Nvidia A6000 GPU (*CF*: 0.17s, *V2C*: 0.12s, *V2M*: 0.16s) plus an additional minute on the CPU for the registration-based alignment.

Table 2: UNetFlow ablation study on the CT validation set ($n = 167$). We evaluate the impact of deep mesh supervision (DMS), voxel branch (VB), and post-processing with the Dice score (mean \pm sd).

DMS	VB	Post-P.	Segmentation Dice			
			Kidneys	Liver	Pancreas	Spleen
-	-	-	0.89 \pm 0.06	0.95 \pm 0.03	0.57 \pm 0.15	0.91 \pm 0.06
-	✓	-	0.89 \pm 0.05	0.95 \pm 0.03	0.61 \pm 0.15	0.91 \pm 0.05
✓	-	-	0.91 \pm 0.04	0.95 \pm 0.01	0.63 \pm 0.14	0.92 \pm 0.03
✓	✓	-	0.91 \pm 0.04	0.96 \pm 0.01	0.61 \pm 0.14	0.93 \pm 0.05
✓	✓	✓	0.93 \pm 0.03	0.96 \pm 0.01	0.73 \pm 0.16	0.94 \pm 0.05

Ablation study We assessed the impact of the deep mesh supervision (DMS), voxel branch (VB), and post-processing in an ablation study on the CT validation set. As can be observed from Table 2, adding the deep mesh supervision (DMS) (cf. Section 2.2) leads to an improvement in segmentation Dice for all organs, except for the liver, where it reduces the variance. The effect is most evident for the pancreas, which is a difficult organ to segment and therefore contains the greatest potential for improvement. Further, adding the voxel segmentation task to UNetFlow enables us to perform the registration-based post-processing step described in Section 2.3. The final method (UNetFlow + post-processing) consistently yields the highest scores in Table 2.

3.2 Topological correctness

Apart from high accuracy, we aim for topologically correct shapes as this is an essential prerequisite for morphological analyses. In parts, the topology of abdominal organs, i.e., being homeomorphic to a sphere, is already carved into the

Table 3: Pre-training on a large CT dataset improves the surface accuracy and leads to faster model convergence on our MRI dataset. We report the average symmetric surface distance (ASSD) and the 90-percentile Hausdorff distance (mean \pm sd) on the MRI test set ($n = 18$).

Method	Pre-tr.	Epochs	Kidneys		Liver	
			ASSD (mm)	HD ₉₀ (mm)	ASSD (mm)	HD ₉₀ (mm)
<i>V2C</i>	-	245	3.24 \pm 1.26	8.54 \pm 4.27	3.55 \pm 1.77	8.91 \pm 6.38
UNetFlow	-	390	2.31 \pm 0.83	7.00 \pm 4.25	2.45 \pm 0.81	6.61 \pm 3.60
UNetFlow	✓	140	1.86 \pm 0.72	5.30 \pm 3.12	2.08 \pm 0.53	5.41 \pm 2.15
			Pancreas		Spleen	
<i>V2C</i>	-	245	5.94 \pm 2.30	16.16 \pm 7.89	3.82 \pm 2.17	11.74 \pm 9.55
UNetFlow	-	390	5.78 \pm 3.09	17.67 \pm 9.65	2.75 \pm 1.32	8.56 \pm 6.79
UNetFlow	✓	140	4.41 \pm 1.87	15.31 \pm 7.73	1.96 \pm 0.61	4.99 \pm 2.16

template we start with. Throughout the deformation, the correspondence to the template is preserved as indicated in supplementary Figure 5. Moreover, the prediction of disconnected shapes is prevented, cf. supplementary Figure 7. A known problem in mesh-based surface reconstruction, however, are self-intersections during the deformation process [16, 5, 6, 4]. Figure 4 shows that there are hardly any self-intersecting faces (SIF) in UNetFlow surfaces (median SIF $< 1e-16\%$ for all organs except the pancreas) and that the number of outliers is lower compared to the baseline methods.

3.3 Transfer learning

We evaluate the performance of UNetFlow on the MRI test set in terms of surface accuracy in Table 3 (further results are in the supplementary material). As can be observed, UNetFlow improves over the strongest baseline from Table 1, *V2C*. Since our MRI dataset is comparably small ($n = 47$ training scans), we assess the effect of pre-training on our CT data and observe that this improves performance while reducing the number of required training epochs.

4 Conclusion

We introduced UNetFlow, a deep diffeomorphic shape deformation approach for multi-organ segmentation. UNetFlow combines surface meshes with voxel segmentation in a single end-to-end trainable neural network. The computed shapes come with vertex-wise correspondence to an input template, which is deformed under the effect of learned multi-resolution deformation fields. Our experiments on CT and MRI data demonstrate the effectiveness of the proposed architecture, yielding realistic organ contours with high accuracy. We believe that our method can be extended to other anatomical structures and modalities and can facilitate various clinical applications that require accurate shape estimation.

Acknowledgments

This research was conducted using the UK Biobank Resource under Application No. 34479. This research was supported by the German Research Foundation and the Federal Ministry of Education and Research in the call for Computational Life Sciences (DeepMentia, 031L0200A). The authors gratefully acknowledge the Leibniz Supercomputing Centre (www.lrz.de) for providing computational resources.

References

- [1] Rafael Palomar, Faouzi A. Cheikh, Bjørn Edwin, Azeddine Beghdadhi, and Ole J. Elle. Surface reconstruction for planning and navigation of liver resections. *Computerized Medical Imaging and Graphics*, 53:30–42, October 2016. 1
- [2] Udaranga Wickramasinghe, Edoardo Remelli, Graham Knott, and Pascal Fua. Voxel2mesh: 3d mesh model generation from volumetric data. pages 299–308, 2020. 1, 2, 4
- [3] Fanwei Kong, Nathan Wilson, and Shawn Shadden. A deep-learning approach for direct whole-heart mesh reconstruction. *Medical Image Analysis*, 74:102222, 2021. 1

- [4] Fabian Bongratz, Anne-Marie Rickmann, Sebastian Pölsterl, and Christian Wachinger. Vox2cortex: Fast explicit reconstruction of cortical surfaces from 3d mri scans with geometric deep neural networks. In *Proceedings of the IEEE/CVF Conference on Computer Vision and Pattern Recognition (CVPR)*, pages 20773–20783, June 2022. [1](#), [2](#), [4](#), [6](#)
- [5] Leo Lebrat, Rodrigo Santa Cruz, Frederic de Gournay, Darren Fu, Pierrick Bourgeat, Jurgen Fripp, Clinton Fookes, and Olivier Salvado. Corticalflow: A diffeomorphic mesh transformer network for cortical surface reconstruction. In *Advances in Neural Information Processing Systems*, 2021. [1](#), [2](#), [3](#), [4](#), [6](#)
- [6] Rodrigo Santa Cruz, Léo Lebrat, Darren Fu, Pierrick Bourgeat, Jurgen Fripp, Clinton Fookes, and Olivier Salvado. Corticalflow++: Boosting cortical surface reconstruction accuracy, regularity, and interoperability. In *Medical Image Computing and Computer Assisted Intervention – MICCAI 2022: 25th International Conference, Singapore, September 18–22, 2022, Proceedings, Part V*, page 496–505, Berlin, Heidelberg, 2022. Springer-Verlag. [1](#), [3](#), [6](#)
- [7] Jun Ma, Yao Zhang, Song Gu, Cheng Zhu, Cheng Ge, Yichi Zhang, Xingle An, Congcong Wang, Qiyuan Wang, Xin Liu, Shucheng Cao, Qi Zhang, Shangqing Liu, Yunpeng Wang, Yuhui Li, Jian He, and Xiaoping Yang. Abdomenct-1k: Is abdominal organ segmentation a solved problem? *IEEE Transactions on Pattern Analysis and Machine Intelligence*, 2021. [1](#), [4](#)
- [8] O. Ronneberger, P. Fischer, and T. Brox. U-net: Convolutional networks for biomedical image segmentation. In *MICCAI*, 2015. [2](#)
- [9] Özgün Çiçek, Ahmed Abdulkadir, Soeren S. Lienkamp, Thomas Brox, and Olaf Ronneberger. 3d u-net: Learning dense volumetric segmentation from sparse annotation. In *Medical Image Computing and Computer-Assisted Intervention – MICCAI 2016*, pages 424–432, Cham, 2016. Springer International Publishing. [2](#)
- [10] Fausto Milletari, Nassir Navab, and Seyed-Ahmad Ahmadi. V-net: Fully convolutional neural networks for volumetric medical image segmentation. pages 565–571, 2016. [2](#)
- [11] Fabian Isensee, Paul F. Jaeger, Simon A. A. Kohl, Jens Petersen, and Klaus Maier-Hein. nnu-net: a self-configuring method for deep learning-based biomedical image segmentation. *Nature methods*, 2020. [2](#)
- [12] Joshua Cates, Shireen Elhabian, and Ross Whitaker. ShapeWorks. In *Statistical Shape and Deformation Analysis*, pages 257–298. Elsevier, 2017. [2](#)
- [13] Thibault Groueix, Matthew Fisher, Vladimir G. Kim, Bryan Russell, and Mathieu Aubry. AtlasNet: A Papier-Mâché Approach to Learning 3D Surface Generation. 2018. [2](#)
- [14] Nanyang Wang, Yinda Zhang, Zhuwen Li, Yanwei Fu, Wei Liu, and Yu-Gang Jiang. Pixel2mesh: Generating 3d mesh models from single rgb images. In *ECCV*, 2018. [2](#)
- [15] Guodong Zeng, Xin Yang, Jing Li, Lequan Yu, Pheng-Ann Heng, and Guoyan Zheng. 3d u-net with multi-level deep supervision: Fully automatic segmentation of proximal femur in 3d mr images. In *Machine Learning in Medical Imaging*, pages 274–282, Cham, 2017. Springer International Publishing. [2](#)
- [16] Kunal Gupta and Manmohan Chandraker. Neural mesh flow: 3d manifold mesh generation via diffeomorphic flows. In *Proceedings of the 34th International Conference on Neural Information Processing Systems, NIPS’20*, Red Hook, NY, USA, 2020. Curran Associates Inc. [3](#), [6](#)
- [17] Nikhila Ravi, Jeremy Reizenstein, David Novotny, Taylor Gordon, Wan-Yen Lo, Justin Johnson, and Georgia Gkioxari. Accelerating 3d deep learning with pytorch3d. *arXiv:2007.08501*, 2020. [3](#)
- [18] Chi Li, M. Zeeshan Zia, Quoc-Huy Tran, Xiang Yu, Gregory Hager, and Manmohan Chandraker. Deep supervision with shape concepts for occlusion-aware 3d object parsing. *2017 IEEE Conference on Computer Vision and Pattern Recognition (CVPR)*, pages 388–397, 2016. [3](#)
- [19] Brian Amberg, Sami Romdhani, and Thomas Vetter. Optimal step nonrigid icp algorithms for surface registration. *2007 IEEE Conference on Computer Vision and Pattern Recognition*, pages 1–8, 2007. [4](#)
- [20] Thomas J. Littlejohns, Jo Holliday, Lorna M. Gibson, Steve Garratt, Niels Oesingmann, Fidel Alfaro-Almagro, Jimmy D. Bell, Chris Boulton, Rory Collins, Megan C. Conroy, Nicola Crabtree, Nicola Doherty, Alejandro F. Frangi, Nicholas C. Harvey, Paul Leeson, Karla L. Miller, Stefan Neubauer, Steffen E. Petersen, Jonathan Sellors, Simon Sheard, Stephen M. Smith, Cathie L. M. Sudlow, Paul M. Matthews, and Naomi E. Allen. The UK biobank imaging enhancement of 100, 000 participants: rationale, data collection, management and future directions. *Nature Communications*, 11(1), May 2020. [4](#)
- [21] German National Cohort (GNC) Consortium. The German National Cohort: aims, study design and organization. *European Journal of Epidemiology*, 29(5):371–382, May 2014. [4](#)

- [22] Fabian Bamberg, Holger Hetterich, Susanne Rospleszcz, Roberto Lorbeer, Sigrid Auweter, Christopher L. Schlett, Anina Schafnitzel, Christiane Bayerl, Andreas Schindler, T. Saam, Katharina Müller-Peltzer, Wieland H. Sommer, Tanja Zitzelsberger, Jürgen Machann, Michael Ingrisch, Sonja Selder, Wolfgang Rathmann, Margit Heier, Birgit Linkohr, Christa Meisinger, Christian Weber, Birgit B. Ertl-Wagner, Steffen Massberg, Maximilian Reiser, and Annette Peters. Subclinical disease burden as assessed by whole-body mri in subjects with prediabetes, subjects with diabetes, and normal control subjects from the general population: The kora-mri study. *Diabetes*, 66:158 – 169, 2016. [4](#)
- [23] Anne-Marie Rickmann, Jyotirmay Senapati, Oksana Kovalenko, Annette Peters, Fabian Bamberg, and Christian Wachinger. AbdomenNet: deep neural network for abdominal organ segmentation in epidemiologic imaging studies. *BMC Medical Imaging*, 22(1), September 2022. [4](#)
- [24] Marc Modat, David Marshall Cash, Pankaj Daga, Gavin P. Winston, John S. Duncan, and Sébastien Ourselin. Global image registration using a symmetric block-matching approach. *Journal of Medical Imaging*, 1, 2014. [4](#)
- [25] Thomas Lewiner, Hélio Lopes, Antônio Wilson Vieira, and Geovan Tavares. Efficient implementation of marching cubes' cases with topological guarantees. *Journal of graphics tools*, 8(2):1–15, 2003. [4](#)

Supplementary material

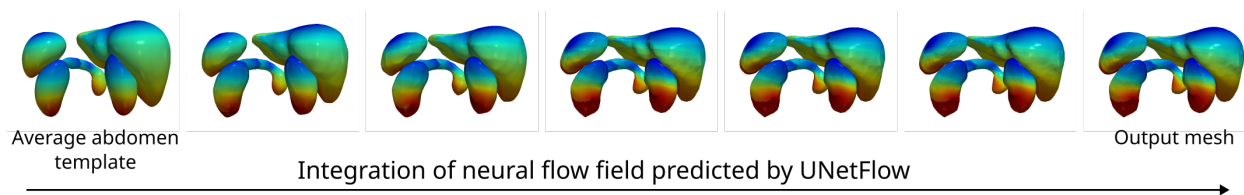


Figure 5: UNetFlow predicts a smooth diffeomorphic deformation of the input template such that vertex correspondences between the template and the reconstructed shapes are established. Colors indicate a unique vertex ID.

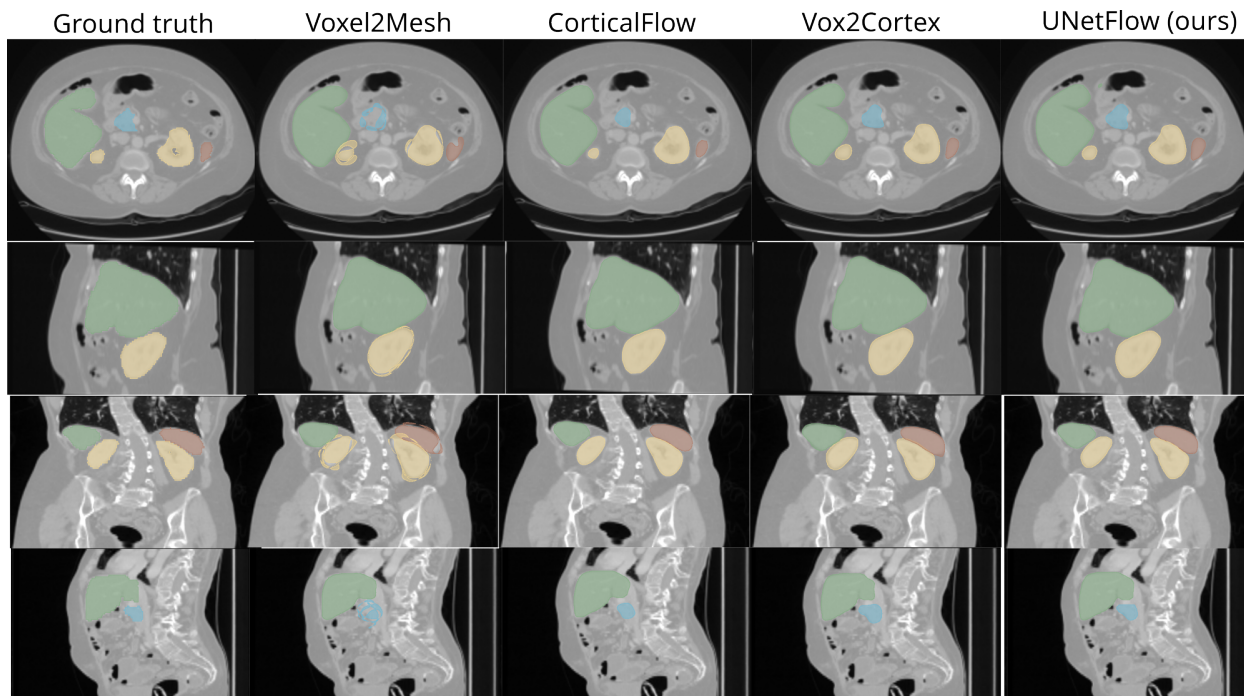


Figure 6: Additional qualitative comparison of mesh-based organ extraction methods.

Table 4: Hyperparameters used in our experiments. We trained and evaluated our models on Nvidia A100 (40GB) and A6000 (48GB) GPUs. Loss weights were tuned for all methods in an initial log-uniform and subsequent uniform range between $1e-4$ and 20 based on the liver.

Optimizer	Learning rate	Batch size	UNet channels	Conv kernel size	Euler steps	Epochs
AdamW	cyclic, $\beta_1 = 0.9,$ $\beta_2 = 0.999$	4	16, 32, 64, 128, 256, 128, 64, 32, 16	$3 \times 3 \times 3$	5	200 (CT) 500 (MRI)

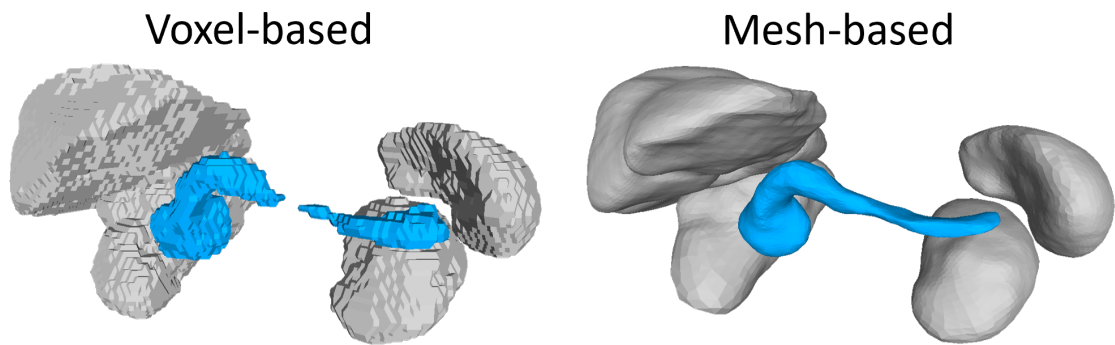


Figure 7: While voxel-based methods are prone to predicting topologically incorrect shapes (pancreas cut into two parts on the left), the connectivity is predefined in UNetFlow (right).